A New Way for IVR Induced by Fast Internal Motion As Revealed by a Jet-Cooled Spectrum of Cyclopentene

L. Lespade and D. Cavagnat*

LPCM, UMR 5308, Université de Bordeaux I, 351 crs de la Libération, 33405 Talence, France

P. Asselin

LADIR/Spectrochimie Moléculaire (UMR CNRS 7075), Université Pierre et Marie Curie, Case courrier 49, Bâtiment F74, 4 place Jussieu, 75253 Paris Cedex 05, France

Received: June 27, 2002

The CH stretching spectra of cyclopentene at 25 K in a molecular beam and at room temperature in a gas cell are measured and compared. These spectra are modeled with an Hamiltonian written in curvilinear coordinates and taking into account, in the adiabatic approximation, the coupling of the CH stretching vibrations with the puckering motion and the angle deformations by Fermi resonance. The curves of the vibrational energy calculated as a function of the puckering coordinate exhibit several crossings. From these crossing points, the vibrational energy can follow different ways. The probability of following one or the other way is discussed and determined from the fit of the two spectra. The presence of some stretching vibrations with an unexpected asymmetrical variation is experimentally evidenced. A correct reproduction of the experimental spectra is obtained.

I. Introduction

The dynamics of molecular vibrations in flexible molecules have been of interest for some time because of their importance in bond-selective photochemistry. Indeed, recently, Diau and collaborators[1] have shown that the ring-puckering motion plays an important role in the S_1 α-cleavage dynamics of cyclobutanone. Cyclopentene constitutes a prototype of non rigid molecules interconverting via a puckering motion between two equivalent non planar ring structures. A great number of experimental investigations[2−13] has evidenced that the puckering potential has a double minimum with a barrier to planarity of some 230 cm^{-1} and that the equilibrium angle between the two dihedral planes of the puckering ring is situated in the range of 22° to 26°. Some mathematical[14−17] analyses have modeled the potential function by a polynomial form $V(X) = V_2 X^2 + V_4 X$,[4] X being the puckering coordinate (Figure 1). Theoretical studies[18,19] reported that a part of the puckering barrier comes from the vibrational zero point energy.

The coupling between the ring-puckering motion and the higher energy vibrations has been pointed out in numerous studies.[7,8,20−24] The CH stretching has received particular attention with the measurement of the CH stretching overtone spectra of the fully hydrogenated cyclopentene[20,21] and through the studies of different selectively deuterated compounds.[22−24] These latter studies have shown that the overtone spectra can be correctly reproduced by treating the coupling between the ring-puckering motion and the other vibrations in the adiabatic approximation and considering the rapid intramolecular vibrational redistribution (IVR) between the CH stretching and the angle deformation vibrations through Fermi resonance couplings. A model Hamiltonian has been written in internal curvilinear coordinates. The same set of effective potential parameters can thus be used for different isotopic derivatives. Part of the used parameters are ab initio calculated, the others are determined from the fit of the overtone spectra of several selectively deuterated compounds. Applying this set of effective potential parameters to the calculation of the CH stretching spectra of the fully hydrogenated cyclopentene appears as a logic achievement of this work.

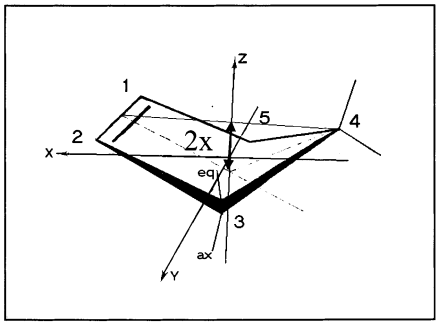

Figure 1. Definition of the ring-puckering coordinate X (in Å).

This paper presents a study of the first excited CH stretching spectra of cyclopentene recorded at low (jet cooled molecular beam) and at room temperature. The discrepancies observed between both spectra are analyzed through the previously developed model and tentatively interpreted.

The structure of the paper will be as follows: After the presentation of the experimental procedure for the molecular beam spectrum measurements, the theoretical basis is briefly recalled. In the last part, the experimental spectra are compared and discussed.

II. Experimental Section

Cyclopentene was purchased at Aldrich and dried with sodium filaments, degassed by the freeze-pump thaw method and transferred under vacuum into a 10 cm path cell. The room-temperature spectrum was then recorded in conditions of thermodynamic equilibrium by standard absorption spectroscopy on a BioRad FTS-60A spectrometer (resolution 0.5 cm^{-1}) between 1200 and 3500 cm^{-1}. The vapor pressure was about 30 Torrs at 296 K.

10.1021/jp021514i CCC: $22.00
Published on Web 09/24/2002

The jet spectra of cyclopentene have been recorded using the molecular beam-FTIR spectrometer device of Paris VI, already described in detail in a previous paper.[25] Briefly, C_5H_8 is seeded in argon at about 10% by sweeping the rare gas over the organic compound cooled at 250 K. Combining the cooling of a stainless steel double-wall hose cylinder containing liquid nitrogen and the heating of an electric resistance, both fitted to an injector, the gas mixture is pre-cooled at about 240 K upstream from the nozzle in order to achieve lower rotational and vibrational temperatures. It is finally expanded through a circular hole of 1 mm diameter and of 2 mm length and evacuated by a 18 $m^3\ h^{-1}$ Varian four stage diffusion pump backed by a 400 $m^3{\cdot}h^{-1}$ Roots pump (Edwards EH 500) and a Leybold D60 (60 $m^3{\cdot}h^{-1}$) rotary vane pump. In these conditions, the background pressure is typically equal to 5×10^{-4} Torrs with a stagnation pressure of 41 Torrs. The supersonic expansion is finally probed by the IR beam of a Bruker IFS 120 HR interferometer which crosses the molecular beam 16 times before being focused on a InSb detector equipped with a cooled band-pass filter centered around the CH stretching region (2900 cm^{-1}) and mounted inside the expansion chamber. A typical spectrum is the Fourier transform of 700 co added interferograms recorded at 0.1 cm^{-1} resolution.

III. Theoretical Approach

The CH stretching vibrations of cyclopentene are perturbed by two main types of coupling: the coupling with the puckering motion and the vibrational couplings between one CH stretching mode and the other vibrations. Previous works[22−24] have shown that the most important and rapid vibrational couplings are the couplings with the other CH stretching modes and with the deformation modes of the angles adjacent to the considered CH bond.

Because of the difference in the time scale of the ring-puckering motion and of the other vibrations, the total Hamiltonian describing the two sorts of motions can be solved with two equations: one describing the vibrations at each molecular position during the ring-puckering motion and the other giving the ring-puckering states. In the second equation, the ring-puckering potential becomes an effective potential,[24] which is the sum of the ground-state ring-puckering potential and of the vibrational energy variation during the motion.

The Schrödinger equation of the ring-puckering motion of fully hydrogenated cyclopentene is as follows

$$-\frac{\hbar^2}{2}\left(\frac{\partial}{\partial X}\right)g(X)\left(\frac{\partial}{\partial X}\right)\psi_n(X) + V^0_{\text{eff}}(X)\psi_n(X) = E_n\psi_n(X) \quad (1)$$

where X is the ring-puckering coordinate, (Figure 1), $g(X)$ the inverse of the reduced mass of the motion. $g(X)$ is calculated by using the basis bisector model of Malloy,[14] and fitted by a polynomial form of order 8. V_{eff} is the effective potential. In the vibrational ground state, it is the sum of the electronic ring-puckering potential and of the zero point vibrational energy. It has been evaluated with a polynomial form of order 4 by fitting the far-infrared and Raman ring-puckering transitions.[26] When the CH bond stretching vibrations are excited, the effective potential $V^1_{\text{eff}}(X)$ is increased by some amount corresponding to the vibrational energy variation during the ring-puckering motion. The resolution of the Schrödinger equation, diagonalized on a basis of 80 harmonic oscillators, gives the energy E^1_n and the wave function $\psi^1_n(X)$ corresponding to the ring-puckering motion state $|1, n\rangle$. The CH stretching spectrum is the sum of all the transitions between the ring-puckering motion states $|0,n\rangle$ in the vibrational ground state and $|1,m\rangle$ in the first CH stretching excited state. The intensity of these transitions are given by

$$I^n|1,m\rangle\leftarrow|0,n\rangle = \nu_{1m,0n}P\left(\int\psi^*_{1m}(X)\langle 0|\bar{\mu}(X)|1\rangle\psi_{0n}(X)dX\right)^2 \quad (2)$$

where $\nu_{1m,0n}$ is the wavenumber of the transition: $(E^1_m - E^0_n/hc)$, P the Boltzmann factor, μ(X) the molecular dipole moment, and $\langle 0|$ and $|1\rangle$ the vibrational wave functions corresponding to the ground and excited vibrational states.

The vibrational energy variation which enters into the effective potential $V^1_{\text{eff}}(X)$ is obtained by the resolution of the vibrational Schrödinger equation for different values of the ring-puckering coordinate X between −0.3 and 0.3 Å by step of 0.01 Å. The vibrational Hamiltonian is analogous to that determined for the selectively deuterated cyclopentene.[24] It is written in curvilinear internal coordinates in order to use the same set of effective vibrational potential parameters for all the isotopic molecules.

Because of the large number of vibrational combination states in a molecule like cyclopentene, even at $\Delta v = 1$, one has to limit the number of degrees of freedom. As a consequence, we only consider those of the three methylene groups. The six methylenic CH bonds are modeled by Morse oscillators

$$\frac{H^0_{vr}}{hc} = \frac{1}{2}\sum_{l}^{3}\sum_{i}^{2}\{g^0_{r_{il}\,r_{il}}p_{r_{il}}p_{r_{il}} + D_{il}(X)[1 - e^{-a_{il}(X)r_{il}}]^2\} + \sum_{il\neq jl'}\left\{\frac{1}{2}g^0_{r_{il}\,r_{jl'}}p_{r_{il}}p_{r_{jl'}} + \frac{1}{2}f_{r_{il}\,r_{jl'}}(X)r_{il}r_{jl'}\right\} \quad (3)$$

In this expression, the r_{il} variables are the CH bond displacement coordinates of the l^{th} methylene group, g^0 the element of the G Wilson kinetic matrix, and f the effective coupling potentials between the CH bonds. $D_{il}(X)$ and $a_{il}(X)$ are the Morse potential parameters and are related to the harmonic wavenumber $\omega_{0il}(X)$ and anharmonicity $\chi_{il}(X)$. Their values have been determined in ref 24 for the methylene groups 3 and 5 (relative to the carbon 3 and 5) and in ref 23 for the methylene group 4 (relative to the carbon 4).

The combination states likely to perturb the CH bond stretching modes by Fermi resonance involve essentially the bending modes at $\Delta v = 1$ and the HCC deformation modes from $\Delta v = 3$ to 6. The anharmonic potentials governing the energy exchange between one CH bond stretching and the deformation modes have been determined in ref 24 for the methylene group 3 or 5 (Figure 1). These potentials parameters are not completely independent from each other. Thus, as the whole set of parameters must be transferred from one molecule to another, all of the angle deformation modes have to be introduced in our model even if effectively only the bending modes combinations enter into resonance with the CH stretching modes at $\Delta v = 1$.

The zero order vibrational Hamiltonian contains terms describing these fifteen angle deformations as anharmonic oscillators

$$\frac{H^0_{v\alpha}}{hc} = \sum_{l=1}^{3}\sum_{i}^{5}\sum_{j}^{5}\left\{\frac{1}{2}(g^0_{\alpha_{il}\,\alpha_{jl}}(X)p_{\alpha_{il}}p_{\alpha_{jl}} + f_{\alpha_{il}\alpha_{jl}}(X)\alpha_{il}\alpha_{jl} + f_{\alpha_{il}\alpha_{il}\alpha_{il}}(X)\alpha^3_{il} + f_{\alpha_{il}\alpha_{il}\alpha_{il}\alpha_{il}}(X)\alpha^4_{il})\right\} \quad (4)$$

where α_{il} are the valence angle displacement coordinates of the

l^{th} methylene group. The G Wilson matrix depends only on the geometry of the molecule. Its elements, corresponding to couplings of angles of different methylene groups, may depend on X. Inside each methylene group, all the angles have been kept equal to their tetrahedral values.

The Fermi resonance interactions of the CH bond stretching modes with the angle deformation combination modes are described by the higher order terms of the Hamiltonian. As in ref 24, only the anharmonic couplings with an important kinetic part, that is to say the couplings between one CH bond stretching mode and the deformation modes of the angles attached to the same carbon atom, are considered. Thus, for each methylene group, the Hamiltonian higher order terms that are retained in the present model are exactly analogous to those of ref 24

$$\frac{H^1_{v-r}}{hc} = \frac{1}{2}\sum_{l=1}^{3}\sum_{i=1}^{2}\sum_{j=1}^{5}\left\{\left(\frac{\partial g^0_{\alpha_{jl}\alpha_{jl}}}{\partial r_{il}}\right)_e r_{il}p^2_{\alpha_{jl}} + \left(\frac{\partial g^0_{r_{il}\alpha_{jl}}}{\partial \alpha_{jl}}\right)_e p_{r_{il}}p_{\alpha_{jl}}\alpha_{jl}\right\} + \frac{1}{2}\sum_{l=1}^{3}\sum_{i=1}^{2}\sum_{j=1}^{5}\left\{\sum_{k=1}^{5}\left[\left(\frac{\partial g^0_{\alpha_{jl}\alpha_{kl}}}{\partial r_{il}}\right)_e p_{\alpha_{jl}}p_{\alpha_{kl}}r_i + \left(\frac{\partial g^0_{r_{il}\alpha_{jl}}}{\partial \alpha_{kl}}\right)_e p_{r_{il}}p_{\alpha_{jl}}\alpha_{kl}\right]\right\} + \frac{1}{2}\sum_{l=1}^{3}\sum_{i=1}^{2}\sum_{j=1}^{5}\sum_{k=1}^{5}\{f_{r_{il}\alpha_{jl}\alpha_{kl}}(X)r_{il}\alpha_{jl}\alpha_{kl}\} \quad (5)$$

where l represents the indices on the three methylene groups, i labels the two CH bonds of each group, and j and k are the five angles of each group. The angles are labeled as in ref 24: $i = 1$ for the bending modes, α_2 and α_3 are the HCC angle deformations adjacent to the first bond r_1, and α_4 and α_5 are the HCC angle deformations adjacent to r_2. The relevant terms in the second-order expansion give

$$\frac{H^2_{v-r}}{hc} = \frac{1}{4}\sum_{l=1}^{3}\sum_{i=1}^{2}\sum_{j=1}^{5}\left\{\left(\frac{\partial^2 g^0_{\alpha_{jl}\alpha_{jl}}}{\partial r^2_{il}}\right)_e r^2_{il}p^2_{\alpha_{jl}} + f_{r_{il}r_{il}\alpha_{jl}\alpha_{jl}}(X)r^2_{il}\alpha^2_{jl}\right\} \quad (6)$$

At the first excited vibrational level, they only give very weak corrections to the Fermi resonance forces.

The effective Hamiltonian is expanded on a basis set whose functions are products of Morse oscillator functions for CH bond stretches and harmonic oscillator wave functions for deformation modes. In the $\Delta v = 1$ polyad, there are 126 possibilities of combination states involving the 6 CH bond stretchings and the 15 angle deformations.

Thus, the zero order Hamiltonian (eqs 3 and 4) gives the unperturbed energy for the state $|v\rangle = |v_{r_{il}}, v_{\delta_l}, v_{w_{jl}}\rangle$ where $\delta_l = \alpha_{1l}$ and $w_{jl} = \alpha_{j+1,l}$ ($l = 1$ to 3; $i = 1,2$; $j = 1$ to 4)

$$E(X,v) = \sum_{l=1}^{3}\left\{\begin{array}{l}\sum_{i=1}^{2}\left(\omega_{0il}(X)\left(v_{r_{il}}+\frac{1}{2}\right) - \chi_{il}(X)\left(v_{r_{il}}+\frac{1}{2}\right)^2\right) \\ \quad + \omega_{\delta_l}(X)\left(v_{\delta_l}+\frac{1}{2}\right) - \chi_{\delta_l}(X)\left(v_{\delta_l}+\frac{1}{2}\right)^2 \\ + \sum_{k=1}^{4}\left(\omega_{w_{kl}}(X)\left(v_{w_{kl}}+\frac{1}{2}\right) - \chi_{w_{kl}}(X)\left(v_{w_{kl}}+\frac{1}{2}\right)^2\right)\end{array}\right. \quad (7)$$

The diagonalization of the vibrational Hamiltonian matrix gives the vibrational energy variations $hc\omega_n(X)$ and the corresponding eigenvectors elements $c_{ni}(X)$ for every X value between -0.3 and 0.3 Å with a step of 0.01 Å. The adiabatic vibrational energy variations $hc\omega_n(X)$ of each normal mode are fitted by a least-squares method to a sixth-order polynomial form and added to $V^0_{eff}(X)$

$$V^{1n}_{eff}(X) = hc\omega_n(X) + V^0_{eff}(X) \quad (8)$$

The transitions between the puckering levels of the different effective potentials $V^0_{eff}(X)$ and $V^{1n}_{eff}(X)$ are then calculated as described previously and added to form the spectrum. As already pointed out, the transition intensities depend on the transition dipole moment $\langle 0|\bar{\mu}(X)|1\rangle$. The dipole moment function can be developed as a Taylor series expansion in the internal stretching displacement coordinates r_{il} around the equilibrium geometry

$$\bar{\mu}(X) = \sum_{l=1}^{3}\sum_{i=1}^{2}\frac{\partial\bar{\mu}(X)}{\partial r_{il}}r_{il} \quad (9)$$

The first dipole moment derivatives can be determined from the ab initio computed atomic polar tensors.[27,28] Their component values are given in Table 1. The transition intensities between $V^0_{eff}(X)$ and $V^{1n}_{eff}(X)$ are then given by

$$I^n|1,k\rangle\leftarrow|0,k'\rangle = \nu_{1k,0k'}P\sum_{l=1}^{3}\sum_{i}^{2}\left(\int\psi^*_{1k}(X)\left\langle 0\left|\frac{\partial\bar{\mu}(X)}{\partial r_{il}}r_{il}\right|1\right\rangle c_{iln}(X)\psi_{0k'}(X)dX\right)^2 \quad (10)$$

where $c_{iln}(X)$ are the eigenvector components of the vibrational normal mode of wavenumber $\omega_n(X)$ corresponding to the six CH stretching Morse oscillators. The effect of the rotation of the entire molecule is taken into account by convoluting each transition by the theoretical asymmetrical top vibration−rotation profile corresponding to each component of the dipole moment variation along the molecular principal axes determined by ab initio calculations. The transitions involving μ_x, μ_y, or μ_z dipole moment components have respectively A, B, or C type band shapes. The B type has a PR profile with no Q branch. The A and C type have a PQR profile characterized by a more intense Q branch and wider PR wings for the C type one. The vibration−rotation profiles have been calculated at different temperatures (25 K and 296 K) by A Perrin.[29] When the cyclopentene molecule is in a flat conformation, it has a C_{2v} symmetry and the symmetry of the normal modes is A_1, B_1, or B_2 depending on the direction of the dipole moment variations (μ_x, μ_z, or μ_y). But when the molecule is in the bent configuration, its symmetry is only C_s and the normal modes involve either μ_y dipole moment component (A″ symmetry) or μ_x and μ_z dipole moment components (A′ symmetry).

The low temperature spectrum exhibits essentially the sharp Q branches of the C type band shape induced by the $\delta\mu_z$ component of the dipole moment variations. Indeed, the $\delta\mu_x(X)$ component is generally too weak for its Q branch to be observed. The intensity of the transitions $|1,k\rangle\leftarrow|0,k'\rangle$ depends on the

TABLE 1: Components of the First Dipole Moment Derivatives (debye/Å) as Calculated from the Atomic Polar Tensor Given by the ab Initio Calculations

C-H bond	$\partial\mu^x/\partial r$	$\partial\mu^y/\partial r$	$\partial\mu^z/\partial r$
α C_3H_9 axial	−0.03805	0.16308	0.21315
α C_3H_8 equatorial	−0.0552	0.22791	−0.12713
α C_3 in plane	−0.04334	0.20168	± 0.18219
β C_4H_{10} axial	−0.1206328	0.	−0.20118
β C_4H_{11} equatorial	−0.23201	0.	0.10041
β in plane	−0.18125	0.	± 0.15137
α C_5H_{13} axial	−0.03805	−0.16308	0.21315
α C_5H_{12} equatorial	−0.0552	−0.22791	−0.12713
α C_5 in plane	−0.04334	−0.20168	± 0.18219

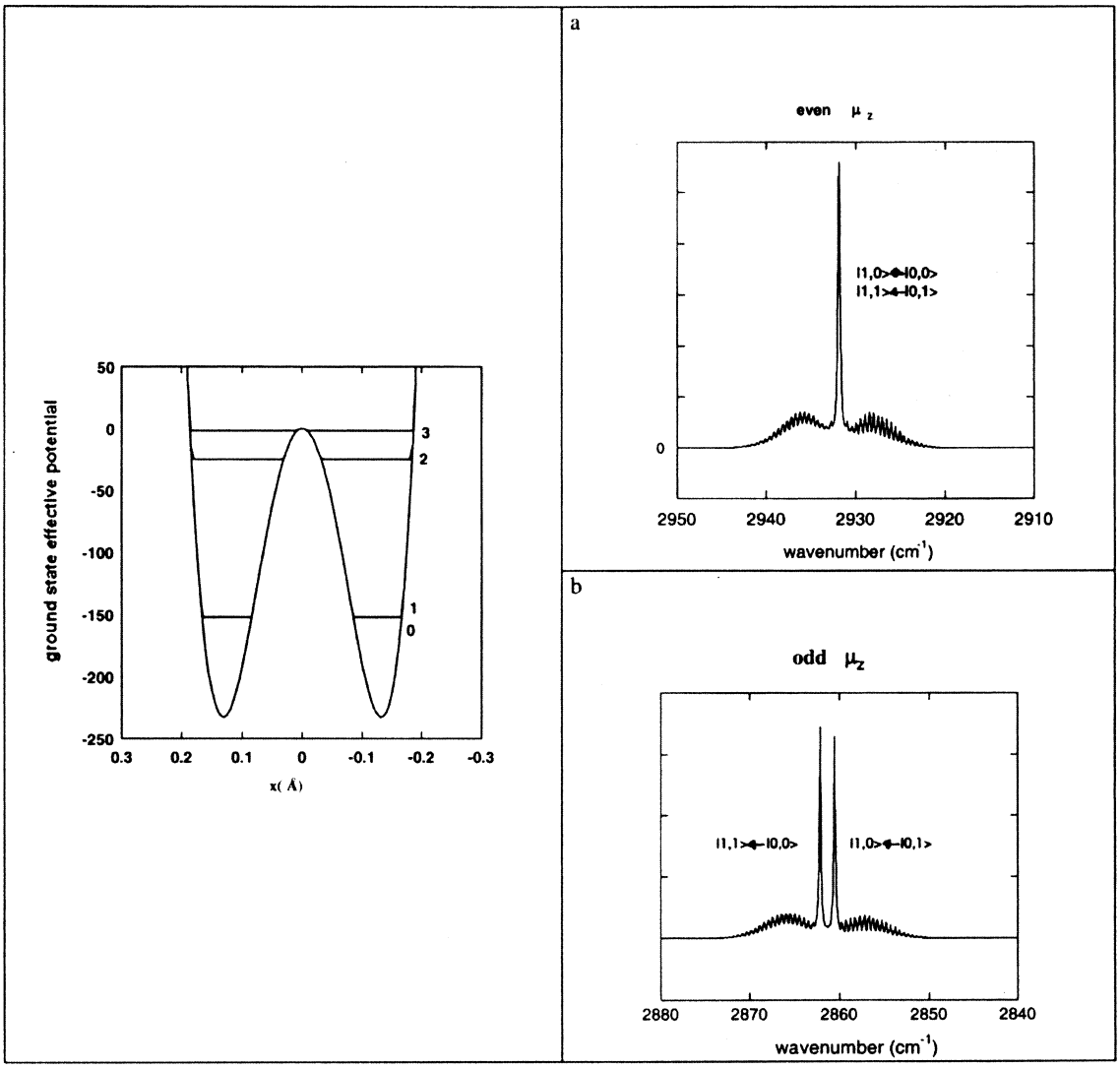

Figure 2. Left: ground-state effective potential of the ring-puckering. In the case of a symmetric vibrationnal energy variation, the effective excited potential is very similar. Right: In case a, is displayed the low temperature theoretical spectrum corresponding to an even μ_z(X). In case b, is displayed the low temperature theoretical spectrum corresponding to an odd μ_z(X). The transitions $|1,0\rangle \leftarrow |0,1\rangle$ and $|1,1\rangle \leftarrow |0,0\rangle$ are indicated.

integration term in eq 10. It has a non zero value only if the product of all its terms is an even function of X.

Thus, for a normal mode of A′ symmetry in the bent conformation (with a AC type band shape) associated to a dipole moment $\delta\mu_z(X) = \sum_i \sum_l c_{iln}(x)\ \partial\mu_z(X)/\partial r_{il}$ which is an even function of X, the intensity of the transitions $|1,k\rangle \leftarrow |0,k'\rangle$ will have a non zero value only if the product of the wave functions ψ_{0k}(X) and $\psi_{1k'}$(X) is also an even function of X. This is the case when $k = k'$. At low temperature, such a normal mode gives rise to a spectrum exhibiting only one C type band shape which corresponds to the two transitions $|1,0\rangle \leftarrow |0,0\rangle$and $|1,1\rangle \leftarrow |0,1\rangle$. Indeed, owing to the small difference between the two effective ring-puckering potentials in the ground and in the first excited vibrational states, these two transitions have approximately the same wavenumber ($\Delta E^0_{0-1} \approx \Delta E^1_{0-1}$) (Figure 2a). On the contrary, if the normal mode has a $\delta\mu_z(X)$ component which is an odd function of X, the product of the wave functions $\psi_{0k}(X)$ and $\psi_{1k'}(X)$ must be also an odd function of X to give rise to transitions with a nonzero intensity, and thus, k' must be equal to $k \pm 1$. At low temperature, this mode appears in the spectrum as formed by two sharp Q branches due to the transitions $|1,0\rangle \leftarrow |0,1\rangle$ and $|1,1\rangle \leftarrow |0,0\rangle$ separated by the sum of the two lowest ring-puckering energy difference ($\Delta E^0_{0-1} + \Delta E^1_{0-1}$).

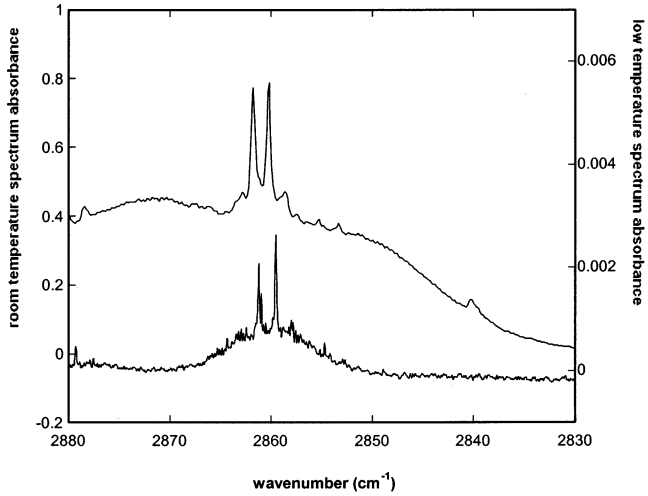

Figure 3. Detail of the experimental infrared spectra corresponding to the lowest energy normal mode. Top: gas-phase room-temperature spectrum obtained with a pressure of 30 Torr. Bottom: low-temperature jet cooled spectrum.

The Figures 2b and 3 give an illustration of such a spectrum pattern. In Figure 3, which represents a detail of the experimental

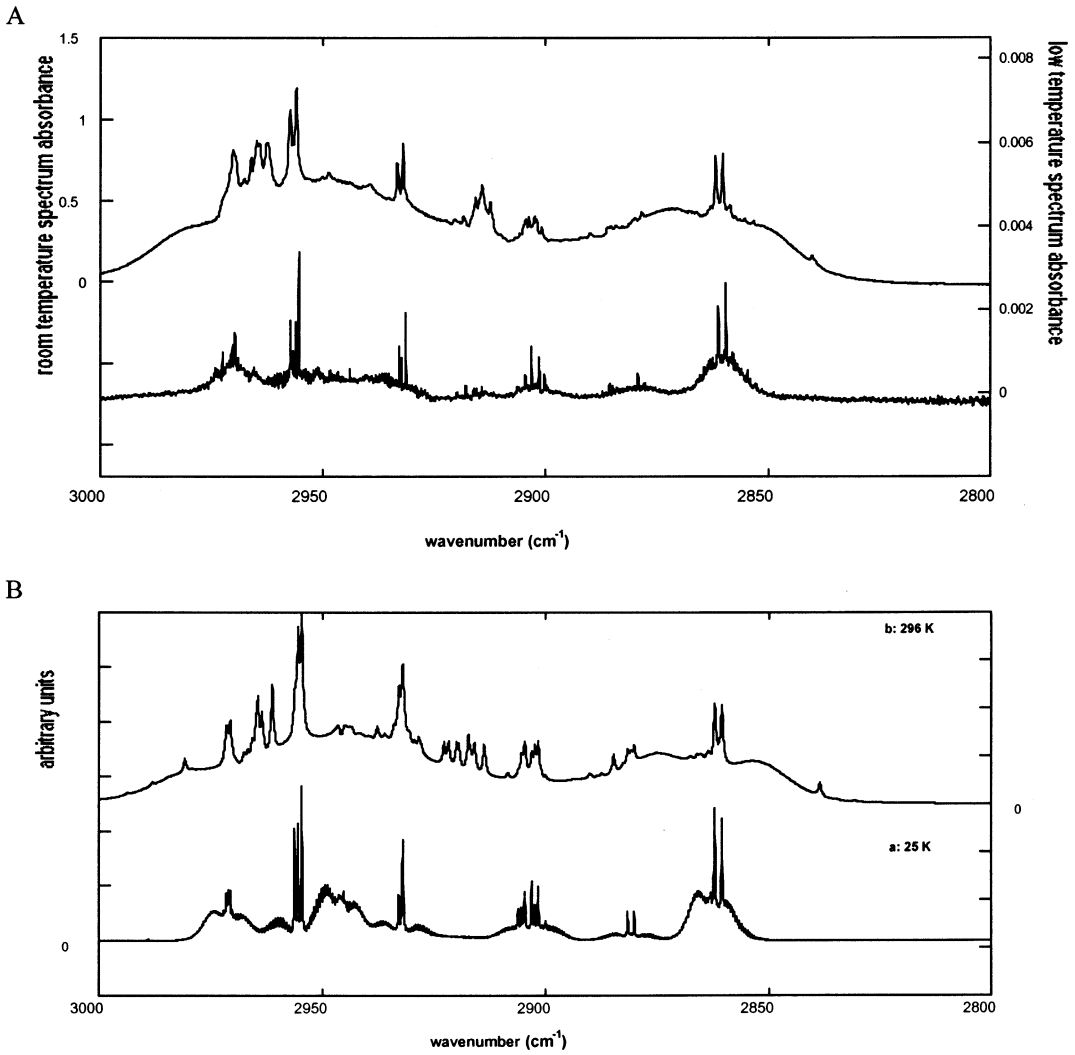

Figure 4. Experimental (A) and theoretical (B) infrared spectra of the CH stretching of cyclopentene C_5H_8. Top (A): gas-phase room-temperature spectrum obtained with a pressure of 30 Torr. Bottom (A): low-temperature jet cooled spectrum. Top (B): the spectrum is calculated with a temperature of 296 K and a probability of 75% for the crossing. Bottom (B): the spectrum is calculated with a temperature of 25 K and equal probabilities for crossing or no crossing.

spectrum corresponding to the lowest energy normal mode, one can notice that, at room temperature, other transitions have non zero intensities: the $|1,3\rangle \leftarrow |0,2\rangle$ and $|1,2\rangle \leftarrow |0,3\rangle$ transitions situated at approximately 25 cm^{-1} apart from the wavenumber ω_n.

IV. Discussion

An overview of the room-temperature and low-temperature spectra of the methylenic CH bond stretching is shown in Figure 4. The cyclopentene molecule possesses six methylenic CH bonds. The CH bond stretching modes are likely to enter into resonance with the six overtone and combination modes of the three CH_2 bending modes. As a consequence, one would expect 12 normal modes in that spectral region, four with B type structure and, thus, with no Q branch and eight with AC type structure. In the low temperature experimental spectrum, one can observe mainly five regions with sharp Q branches. Only one, around 2860 cm^{-1}, also observed in the room-temperature spectrum, has the expected pattern of a normal mode of A−C symmetry and odd $\delta\mu_z(X)$. The other spectral regions are more complex and some differences can be observed between the two spectral features.

The room-temperature spectrum exhibits some extra hot bands around 2965 cm^{-1} and 2915 cm^{-1}. For symmetrical ring-puckering potentials, the most intense hot bands can be due either to the $|1,2\rangle \leftarrow |0,3\rangle$ or $|1,3\rangle \leftarrow |0,2\rangle$ transitions (in the case of an odd function for $\delta\mu_z(X)$) which are situated approximately at 25 cm^{-1} apart from the main $|1,0\rangle \leftarrow |0,1\rangle$ transition (for example the small peaks at 2878 and 2842 cm^{-1} in Figure 3) or to the $|1,k\rangle \leftarrow |0,k\rangle$ transitions (in the case of an even function of $\delta\mu_z(X)$) which are situated in the vicinity of the fundamental transition. The observed extra hot bands around 2965 and 2915 cm^{-1} cannot correspond to such $|1,k\rangle \leftarrow |0,k\rangle$ transitions as they are not in the vicinity of the low-temperature bands nor to the $|1,2\rangle \leftarrow |0,3\rangle$ or $|1,3\rangle \leftarrow |0,2\rangle$ transitions as they have complex features. These hot bands pattern presents similar characters to the central features observed in the CH stretching spectrum of the monohydrogenated cyclopentene[30] which are due to transitions issued from excited ring-puckering levels lying above the barrier. They are the signature of asymmetry of the effective potentials. Because of the cyclopentene symmetry, the effective puckering potential is symmetric in the ground vibrational state and can only takes asymmetrical character in the excited vibrational state from the additional vibrational energy variation

TABLE 2: Effective Parameters Used in the Modeling of the Spectra (X is in Å)

local parameters for the CH(CD) bond stretching modes (cm^{-1})

$\omega_0(X) = 3038.6 + 273X + 109X^2 - 4732X^3 - 3389X^4 + 4369\,X^5 + 111150X^6$	for the α-CH stretches (l=1,3)
$\omega_0(X) = 3073.5 + 135X - 338X^2 - 2208X^3 + 21000X^4$	for the β-CH stretches (l=2)
$\chi\,(X) = 64.6 - 2.5X - 34.5X^2 - 44.5X^3 + 1250X^4$	for the α-CH stretches (l=1,3)
$\chi\,(X) = 62.6 - 5.5X - 69.5X^2 - 89.0X^3 + 2500X^4$	for the β-CH stretches (l=2)

CH stretching−CH stretching interactions f_{rirj} (in mdyn/Å)

	$0.05 + 2.08X^2$	$0.004 + 0.1125X - 0.0347X^2$	$0.0205 - 0.054X + 0.0104X^2$	$-0.0054 - 0.0167X + 0.111X^2$	$-0.008 + 0.903X^2$
$0.05 + 2.08X^2$		$0.0205 + 0.054X + 0.0104X^2$	$0.004 - 0.1125X - 0.0347X^2$	$-0.008 + 0.903X^2$	$-0.0054 + 0.0167X + 0.111X^2$
$0.004 + 0.1125X - 0.0347X^2$	$0.0205 + 0.054X + 0.0104X^2$		$0.059 + 0.5555X^2$	$0.004 + 0.1125X - 0.0347X^2$	$0.0205 + 0.054X + 0.0104X^2$
$0.0205 - 0.054X + 0.0104X^2$	$0.004 - 0.1125X - 0.0347X^2$	$0.059 + 0.5555X^2$		$0.0205 - 0.054X + 0.0104X$	$0.004 - 0.1125X - 0.0347X^2$
$-0.0054 - 0.0167X + 0.111X^2$	$-0.008 + 0.903X^2$	$0.004 + 0.1125X - 0.0347X^2$	$0.0205 - 0.054X + 0.0104X^2$		$0.05 + 2.08\,X^2$
$-0.008 + 0.903X^2$	$-0.0054 + 0.0167X + 0.111X^2$	$0.0205 + 0.054X + 0.0104X^2$	$0.004 - 0.1125X - 0.0347X^2$	$0.05 + 2.08X^2$	

CH stretching−CH stretching interactions f_{rirj} (in mdyn/Å) in the equilibrium conformation (the ab initio constants are indicated in parentheses)

	0.08	0.017	0.0141	−0.0058	0.005
0.08 *(0.079)*		0.027	−0.01	0.005	−0.001
0.017 *(−0.009)*	0.027 *(0.026)*		0.067	0.017	0.027
0.0141 *(0.022)*	−0.01 *(0.003)*	0.067 *(0.063)*		0.0141	−0.01
−0.0058 *(0.001)*	0.005 *(0.002)*	0.017	0.0141		0.08
0.005 *(0.002)*	−0.001 *(0.004)*	0.027	−0.01	0.08	

parameters for the bends in cm^{-1} *(δ labels the HCH or HCD deformation and* w_i *the HCC bends i = 1,4; see Figure 2 of ref 24):*

$\omega_{\delta l}(X) = 1290-30X^2$	for the α-HCH bend (l=1,3)	
$\chi_{\delta l}(X) = 4$		
$\omega_{\delta l}(X) = 1308.5 - 300X^2 + 4000X^4$	for the β-HCH bend (l=2)	
$\chi_{\delta l}(X) = 2$		
$f_{r\delta l}\delta_l(X) = -0.28 + 0.17\,X + 5.55X^2$ (in mdyn)	for the α-HCH bend (l=1,3)	
$f_{rr\delta l}\delta_l(X) = -1.65$ (in mdyn/Å)		
$f_{r\delta l}\delta_l(X) = -0.03-0.18X + 3.50X^2$ (in mdyn)	for the β-HCH bend (l=2)	
$f_{rr\delta l}\delta_l(X) = -1.65$ (in mdyn/Å)		
$\omega_{wi,l}(X) = 1123 + 82X - 150X^2 - 1000X^3 + 4000X^4$	i = 1,2	
$\omega_{wi,l}(X) = 1123-52X - 150X^2 - 1000X^3 + 4000X^4$	i = 3,4	for the α-HCC deformation
$\chi_{wi,l}(X) = 8$	l = 1,3	
$\omega_{wi,l}(X) = 1110 + 52X - 150X^2 + 4000X^4$	i = 1,2	
$\omega_{wi,l}(X) = 1110-52X - 150X^2 + 4000X^4$	i = 3,4	for the β-HCC deformation
$\chi_{wi,l}(X) = 8$	l = 2	

For α-HCC deformation modes (l=1,3):

$f_{r_1w_1w_1} = f_{r_1w_2w_2} = -0.545-0.21X$	$f_{r_2w_3w_3} = f_{r_2w_4w_4} = -0.545 + 0.21X$	(in mdyn)
$f_{r_1w_3w_3} = f_{r_1w_4w_4} = -0.82X$	$f_{r_2w_1w_1} = f_{r_2w_2w_2} = +0.82X$	(in mdyn)
$f_{r_1\delta w_1} = f_{r_1\delta w_2} = 0.385 + 0.3X$	$f_{r_2\delta w_3} = f_{r_2\delta w_4} = 0.385-0.3X$	(in mdyn)
$f_{r_1\delta w_3} = f_{r_1\delta w_4} = -0.15-0.4X$	$f_{r_2\delta w_1} = f_{r_2\delta w_2} = -0.15 + 0.4X$	(in mdyn)
$f_{r_1w_1w_2} = -0.82-0.45X$	$f_{r_2w_3w_4} = -0.82 + 0.45X$	(in mdyn)
$f_{r_1w_1w_3} = f_{r_1w_2w_4} = 0$	$f_{r_2w_1w_3} = f_{r_2w_2w_4} = 0$	(in mdyn)
$f_{r_1r_1w_1w_1} = f_{r_1r_1w_2w_2} = 0.9 + 0.03X$	$f_{r_2r_2w_3w_3} = f_{r_2r_2w_4w_4} = 0.9-0.03X$	(in mdyn/Å)

For β-HCC deformation modes (l=2):

$f_{r_1w_1w_1} = f_{r_1w_2w_2} = -0.49-2.2X$	$f_{r_2w_3w_3} = f_{r_2w_4w_4} = -0.49 + 2.2X$	(in mdyn)
$f_{r_1w_3w_3} = f_{r_1w_4w_4} = 0$	$f_{r_2w_1w_1} = f_{r_2w_2w_2} = 0$	(in mdyn)
$f_{r_1\delta w_1} = f_{r_1\delta w_2} = 0.485-0.3X$	$f_{r_2\delta w_3} = f_{r_2\delta w_4} = 0.485 + 0.3X$	(in mdyn)
$f_{r_1\delta w_3} = f_{r_1\delta w_4} = -0.05$	$f_{r_2\delta w_1} = f_{r_2\delta w_2} = -0.05$	(in mdyn)
$f_{r_1w_1w_2} = -0.28-0.7X$	$f_{r_2w_3w_4} = -0.28-0.7X$	(in mdyn)
$f_{r_1w_1w_3} = f_{r_1w_2w_4} = -0.35$	$f_{r_2w_1w_3} = f_{r_2w_2w_4} = -0.35$	(in mdyn)
$f_{r_1r_1w_1w_1} = f_{r_1r_1w_2w_2} = 0.9 + 0.03X$	$f_{r_2r_2w_3w_3} = f_{r_2r_2w_4w_4} = 0.9 - 0.03X$	(in mdyn/Å)

$hc\omega_n(X)$. This implies that some vibrational energy curves present asymmetrical variation versus the ring-puckering coordinate.

A. Calculation Parameters. The vibrational potential parameters describing the couplings between the CH bond stretchings related to the carbon 3 or 5 and the angle deformation modes attached to the same carbon atom have been determined in the bent conformations[24] in former studies of the 1,2,3,4,4,5,5d_7-cyclopentene and 4,4,5,5d_4-cyclopentene molecules. The values of these parameters for the flat configuration ($X = 0$) are not easily accessible experimentally because the spectra are essentially due to transitions issued from the two lowest ring-puckering levels localized in the bottom of the potential wells. Indeed, in the overtone spectra, the ring-puckering effective potential barrier is too high for the transitions issued from the ring-puckering levels above the potential barrier to have a significant intensity. The only experimental indications for these parameters at $X = 0$ would be contained in the first excited CH bond stretching spectra of the selectively deuterated compounds. The analysis of the spectrum of cyclopentene-d_4 [24] has shown that it is not very sensitive to the flat position. The spectrum of 1,2,3,4,4,5,5d_7-cyclopentene possesses hot bands and gives indications on the CH stretch harmonic wavenumber $\omega_0(0)$ but not on the other parameters and in particular on the angle deformation parameters since this spectrum is not perturbed by Fermi resonance. In ref 30, the vibrational energy variation

$\omega_0(X)$ of the CH stretching of the monohydrogenated cyclopentene has been slightly modified with respect to the ab initio determination used in ref 24 for a better reproduction of the transitions implying the levels above the barrier height. In the present study, all the potential parameters used in ref 24 have been kept except for $\omega_{0il}(X)$ ($l = 1,3$) determined in ref 30. The other parameters, not relevant in ref 24, correspond to the CH bonds related to the carbon 4 (apex; $l = 2$) and to the coupling of the CH bond stretching or angle deformation modes related to carbon 4 and 3 or 5. For the apex CH bond stretching, the values of $\omega_{0i2}(X)$ and $\chi_{i2}(X)$ determined from the study of the monohydrogenated 1,2,3,3,4,5,5d$_7$-cyclopentene[7,31] have been used. The CH bond coupling, angle deformation coupling and Fermi resonance coupling parameters have been fitted for a good reproduction of the spectra. The two first are harmonic couplings and would normally be obtained from ab initio calculations. Unfortunately, these ab initio parameters have often unphysical values because the large amplitude ring-puckering motion is treated by Gaussian software as an harmonic motion for the determination of the harmonic force constants. This leads to a pollution of the force constants of the vibrations the more linked to the ring-puckering motion. The CH−CH bond coupling constants determined in this work and presented in Table 2 have equilibrium conformation values comparable to those determined by ab initio calculations.[32] On the contrary, the ab initio values of the coupling force constants for the angle deformation modes have no physical scale of magnitude. Thus, the corresponding coupling parameters have been fitted for the equilibrium conformation in order to reproduce the deformation mode absorption of several isotopic derivatives already studied in the litterature.[33]

In the absence of some experimental information about the values of these parameters for the flat conformation, they have been evaluated according to some tendency indicated by the ab initio calculations. In particular, the angle deformation couplings have been slightly modified to reproduce a blue shift of the wagging wavenumbers.

Once the parameters obtained for the two configurations at the equilibrium and for $X = 0$, their variations have been fitted by a polynomial form of order 2 and displayed in Table 2. The set of parameters used in this model is maybe not unique. However, it has been successful in describing the spectra of different isotopic species of cyclopentene.

B. Results. The adiabatic vibrational energy variations of the A′ symmetry normal modes obtained for every X value between −0.3 and 0.3 Å by step of 0.01 Å by diagonalization of the vibrational Hamiltonian matrixes, are displayed in Figure 5. In this diagram, four crossings can be noticed: two at $X = 0$ and $E = 2965$ and 2920 cm^{-1}, and two near the positions $X = \pm 0.13$ Å (which correspond to the ground-state effective potential minima) and $E = 2905$ cm^{-1}.

If we consider for example the spectral region between 2950 and 2980 cm^{-1}, which corresponds to the two upper curves of Figure 5, the theoretical spectrum can be calculated by considering either two symmetrical non crossing (spectrum 1) (Figure 6 case b) or two asymmetrical curves resulting from the crossing at $X = 0$ of the previously considered symmetrical curves (spectrum 2) (Figure 6 case a).

At low temperature, spectrum 1 is composed of one doublet at 2955 cm^{-1} and a peak at 2971 cm^{-1}. The single peak at 2971 cm^{-1} corresponds to the higher energy curve of Figure 5 related to a normal mode whose $\delta\mu_z(X)$ dipolar moment component is an odd function of X. As explained in section III, this peak is due to the two transitions $|1,k\rangle \leftarrow |0,k\rangle$ with $k = 0$ and $k = 1$.

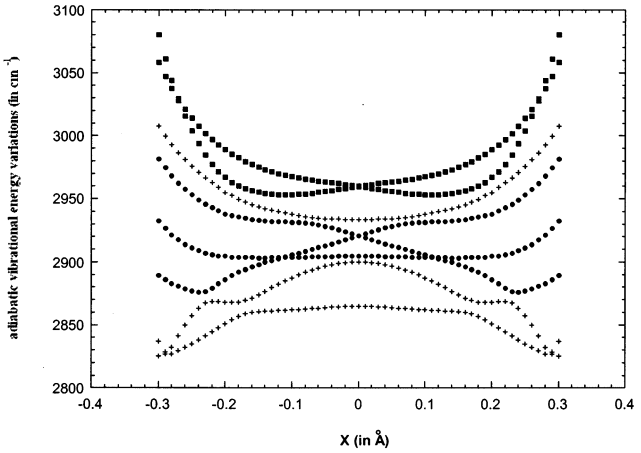

Figure 5. Calculated vibrational energy variations for the normal modes of A′ symmetry.

When temperature is increased, transitions with $k > 1$ gain some intensity but appear in the vicinity of the two first transitions. The doublet around 2955 cm^{-1} corresponds to the second curve related to a normal mode whose $\delta\mu_z(X)$ dipolar moment component is an even function of X. This doublet is formed by the two transitions $|1,0\rangle \leftarrow |0,1\rangle$ and $|1,1\rangle \leftarrow |0,0\rangle$ split by an energy difference equal to $\Delta E^0_{0-1} + \Delta E^1_{0-1}$. At higher temperature, the hot bands expected for such a mode ($|1,2\rangle \leftarrow |0,3\rangle$ or $|1,3\rangle \leftarrow |0,2\rangle$) would be observed near 2930 and 2980 cm^{-1}.

In the case of spectrum 2, the potential and the dipole moment functions present no more symmetry versus X. Thus, a lot of transitions are permitted. The doublet around 2955 cm^{-1} is now due to the two transitions $|1,0\rangle \leftarrow |0,1\rangle$ and $|1,0\rangle \leftarrow |0,0\rangle$ split by an energy difference equal to ΔE^0_{0-1} ($\approx$ the half of the spacing of the doublet in the symmetrical case). An equally spaced doublet is also observed at 2971 cm^{-1}. It is due to the $|1,1\rangle \leftarrow |0,1\rangle$ and $|1,1\rangle \leftarrow |0,0\rangle$ transitions. Indeed, the asymmetry of the effective potential of the first excited CH stretching state brought by the addition of the vibrational energy variation induces a large splitting of the two lowest ring-puckering levels ΔE^1_{0-1}. This splitting corresponds to the energy difference between the two doublets.[7,8,30] At higher temperature, the hot bands associated to this asymmetrical potential give rise to a complex structure around 2965 cm^{-1} between the frequency of the two doublets.

A similar analysis can be done for the lower energy crossing curves of Figure 5.

The analysis of the molecular beam experimental spectrum shows that characteristics of the both types of spectra (with symmetrical and asymmetrical potentials) can be observed (Figures 4 and 6). Furthermore, the presence of hot bands around 2965 and 2915 cm^{-1} when temperature increases indicates that crossings between some vibrational energy curves are expected.

Thus, by modeling the CH stretching spectrum of cyclopentene, it has been supposed that, for each crossing, there is an equal probability for the adiabatic vibrational energy curves to have a symmetrical or an asymmetrical variation. At low temperature (25 K), the so calculated spectrum compares rather well with the experimental one (Figures 4 and 6). But, at room temperature, an equal probability gives too weak hot bands near 2965 and 2945 cm^{-1}. In addition, the hot bands expected for a symmetric potential case, clearly observable in the room-temperature spectrum at 2842 and 2878 cm^{-1} for the mode near 2860 cm^{-1} are not visible at 2980.5 cm^{-1} for the two transitions at 2955.5 and 2957 cm^{-1}. This indicates that the asymmetrical

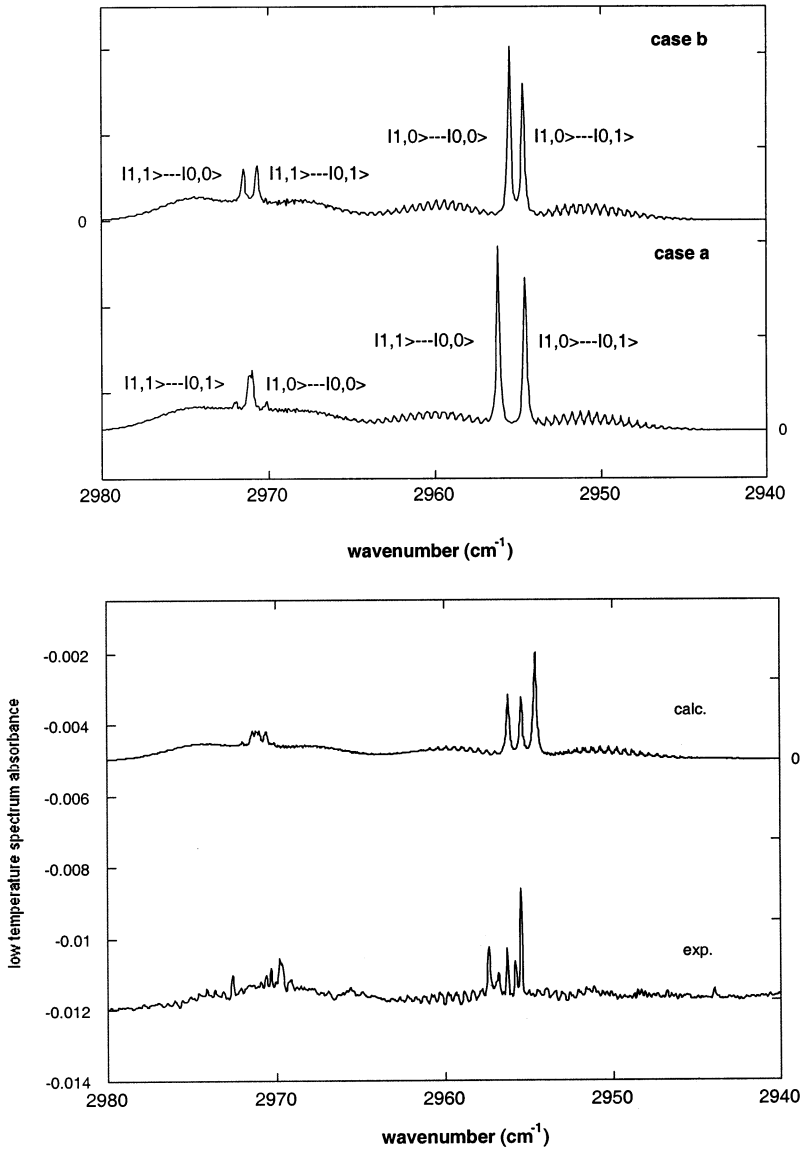

Figure 6. (Top) Theoretical spectra corresponding to the two highest energy adiabatic curves of Figure 5. Case a displays the sum of the spectra corresponding to the two symmetric curves, case b that of the two asymmetrical curves with a crossing at $x = 0$. (Bottom) Comparison between the experimental and the calculated spectra at low temperature. The calculated spectrum is the sum of the two spectra a and b displayed above.

vibrational energy variation may be favored when temperature is increasing.

A better agreement with the room-temperature spectrum is reached by increasing the probability of the asymmetrical case till 75%. The overall shape of these hot bands is not still very well reproduced. In particular, the upper transitions are too intense. They correspond to transitions from ring-puckering levels situated at the vicinity of the potential barrier. In all of the previous studies, these transitions are also calculated too intense.[7,8,30] This defect may be due to a bad reproduction of the form of the top of the barrier of the ring-puckering potential.

The less good reconstruction of the clump of peaks near 2915 cm^{-1} may also results from the greater number of possible crossings for the corresponding vibrational curves and from the bad estimation of the probabilities at each crossing.

Conclusion

The CH stretching spectra of cyclopentene at low temperature in a molecular beam and at room temperature have been compared and analyzed. The modeling of the spectra, even with the adiabatic approximation, implies a lot of effective parameters since a lot of vibrations are involved in the CH stretching modes. To reduce their numbers, all of the parameters obtained from the previous studies on isotopic derivatives of cyclopentene have been used. The experimental spectra evidence the existence of crossings of the adiabatic vibrational energy variation curves. To our knowledge, it is the first time that such crossings are experimentally observed at this energy, in normal mode regime. Some "avoided crossings" have been enlightened in aniline and H_2O_2 rovibrationnal state calculations.[34,35] They are characteristic of very congested spectra at high energy. In these works, a technique of diabatic rotations is used to force the crossings of the adiabatic curves to favor the local mode regime which prevails at these energies. In the case of cyclopentene molecule, a fine analysis of the low temperature spectrum indicates that, when there is a crossing between two curves, the vibrational energy may vary in a symmetrical or an asymmetrical way with approximately an equal probability. It can be noticed that the fine structure of the low temperature spectrum indicates the overall form of the vibrational potential, even if only the lowest

transitions from the first puckering levels in the bottom of the potential wells are involved. Indeed, the bands are characteristic of the symmetry of the effective potential and of the vibrational dipole moment variation. The room-temperature spectrum indicates that, at higher temperature, the crossings (asymmetrical effective potentials) are favored.

In conclusion, the modeling of the cyclopentene spectra with effective parameters and within the adiabatic approximation frame enables to understand a large number of the fine structures of the low-temperature spectrum. But it fails in giving predictions of the probabilities of crossing between the adiabatic curves when there are different possibilities for the vibrational energy variation. Maybe a time dependent wave packet motion model will be able to give this information.

References and Notes

(1) Diau, E. W. G.; Kötting, C.; Zewail, A. H. *Chem. Phys. Chem.* **2001**, *2*, 294.
(2) Laane, J.; Lord, R. C. *J. Chem. Phys.* **1967**, *47*, 4941.
(3) Ueda, T.; Shimanouchi, T. *J. Chem. Phys.* **1967**, *47*, 5018.
(4) Green, W. H. *J. Chem. Phys.* **1970**, *52*, 2156.
(5) Durig, J. R.; Carreira, L. A. *J. Chem. Phys*. **1972**, *56*, 4966.
(6) Bauman, L. E.; Killough, P. M.; Cooke, J. M.; Villareal, J. R.; Laane, J. *J. Phys. Chem*. **1982**, *86*, 2000, and references therein.
(7) Cavagnat, D.; Banisaeid-Vahedie, S.; Grignon-Dubois, M. *J. Phys. Chem*. **1991**, *95*, 5073. Cavagnat, D.; Banisaed-Vahedie, S. *J. Phys. Chem*. **1991**, *95*, 8529.
(8) Cavagnat, D.; Banisaeid-Vahedie, S.; Lespade, L.; Rodin, S. *J. Chem. Soc., Faraday Trans.* **1992**, *88*, 1845.
(9) Davis, M. I.; Muecke, J. W. *J. Phys. Chem*. **1970**, *74*, 1104.
(10) Rathjens, G. W. *J. Chem. Phys.* **1962**, *36*, 2401.
(11) Butcher, S. S.; Costain, C. C. *J. Mol. Spectrosc*. **1962**, *15*, 40.
(12) Scharpen, L. H. *J. Chem. Phys.* **1968**, *48*, 3552.
(13) Lopez, J. C.; Alonso, J. L.; Charro, M. E.; Wlodarczak, G.; Demaison, J. *J. Mol. Spectrosc.* **1992**, *143*, 1555.
(14) Malloy, T. B. *J. Mol. Spectrosc.* **1972**, *44*, 504.
(15) Malloy, T. B.; Carreira, L. A. *J. Chem. Phys*. **1979**, *71*, 2488.
(16) Pyka, J. *J. Mol. Spectrosc*. **1992**, *151*, 423.
(17) Sztraka, L. *Spectrochim. Acta* **1992**, *48A*, 65.
(18) Champion, R.; Godfrey, P. D.; Bettens, F. L. *J. Mol. Struct*. **1991**, *147*, 488.
(19) Allen, W. D.; Csaszar, A. G.; Horner, D. A. *J. Am. Chem. Soc*. **1992**, *114*, 6834.
(20) Henry, B. R.; Hung, I. F.; MacPhail, R. A.; Strauss, H. L. *J. Am. Chem. Soc*. **1980**, *102*, 515.
(21) Wong, J. S.; MacPhail, R. A.; Moore, C. B.; Strauss, H. L. *J. Phys. Chem*. **1982**, *86*, 1478.
(22) Rodin-Bercion, S.; Cavagnat, D.; Lespade, L.; Maraval, P. *J. Phys. Chem*. **1995**, *99*, 3005.
(23) Lespade, L.; Rodin-Bercion, S.; Cavagnat, D. *J. Phys. Chem*. **1997**, *101*, 2568.
(24) Lespade, L.; Rodin-Bercion, S.; Cavagnat, D. *J. Phys. Chem.* **2000**, *104*, 9880.
(25) Asselin, P.; Soulard, P.; Manceron, L.; Boudon, V.; Pierre, G. *J. Mol. Struct*. **2000**, *145*, 517.
(26) Villareal, J. R.; Bauman, L. E.; Laane, J. *J. Phys. Chem*. **1976**, *80*, 1172.
(27) Biarge, J. F.; Herrantz, J.; Morcillo, J. *J. Annu. Rev. Soc. Esp. Fis. Quim*. **1961**, A57
(28) Person, W. B.; Newton, J. H. *J. Chem. Phys*. **1974**, *61*, 1040.
(29) Perrin, A. Private communication.
(30) Cavagnat, D.; Lacome, N.; Lespade, L. *J. Phys. Chem. A* **2002**, *106*, 9460.
(31) Lapouge, C.; Cavagnat, D.; Gorse, D.; Pesquer, M. *J. Phys. Chem*. **1995**, *99*, 2996.
(32) Frisch, M. J.; Head-Gordon, M.; Schlegel, H. B.; Raghavachari, K.; Binkley, J. S.; Gonzalez, C.; Defrees, D. J.; Fox, D. J.; Whiteside, R. A.; Seeger, R.; Melius, C. F.; Baker, J.; Martin, R.; Kahn, L. R.; Steward, J. J. P.; Fluder, E. M.; Topiol, S.; Pople, J. A. Gaussian Inc. , Pittsburgh, PA, 1988.
(33) Villareal, J. R.; Laane, J.; Bush, S. F.; Harris, W. C. *Spectrochim. Acta* **1979**, *35A*, 331.
(34) Fehrensen, B.; Luckhaus, D.; Quack, M. *Zeitschrift für Phys. Chem.* **1999**, *209*, 1; *Chem. Phys*. *Lett*. **1999**, *300*, 312.
(35) Luckhaus, D. *J. Chem. Phys*. **2000**, *113*, 1329.